

Dynamical Response of Nanomechanical Oscillators in Immiscible Viscous Fluid for *In Vitro* Biomolecular Recognition

Jerome Dorignac,^{1,2} Agnieszka Kalinowski,^{3,*} Shyamsunder Erramilli,^{1,3} and Pritiraj Mohanty¹

¹*Department of Physics, Boston University, 590 Commonwealth Avenue, Boston, Massachusetts 02215, USA*

²*College of Engineering, Boston University, 44 Cummington Street, Boston, Massachusetts 02215, USA*

³*Department of Biomedical Engineering, Boston University, 48 Cummington Street, Boston, Massachusetts 02215, USA*

(Received 11 February 2006; published 11 May 2006)

Dynamical response of nanomechanical cantilever structures immersed in a viscous fluid is important to *in vitro* single-molecule force spectroscopy, biomolecular recognition of disease-specific proteins, and the study of microscopic protein dynamics. Here we study the stochastic response of biofunctionalized nanomechanical cantilever beams in a viscous fluid. Using the fluctuation-dissipation theorem we derive an exact expression for the spectral density of displacement and a linear approximation for resonance frequency shift. We find that in a viscous solution the frequency shift of the nanoscale cantilever is determined by surface stress generated by biomolecular interaction with negligible contributions from mass loading due to the biomolecules.

DOI: 10.1103/PhysRevLett.96.186105

PACS numbers: 81.07.-b, 45.10.-b, 82.70.Dd, 83.10.Mj

From single-molecule force spectroscopy [1] to biomolecular recognition of disease-specific proteins such as cancer antigens [2], micron-sized cantilevers have proved to be fundamental to the ultrasensitive detection of small forces. Usually, forces are detected by measuring the deflection of the cantilever. In the dynamic case, shift in the resonance frequency of the cantilever is used to infer the magnitude of force. Micromachining techniques now enable commercial production of such cantilevers with dimensions on the order of 100 μm as well as their routine use in force spectroscopy.

Decreasing the cantilever dimensions to submicron or nanometer scales increases resonance frequency to the megahertz-gigahertz range. The resultant increase in the dynamic range and the measurement speed can provide a better tool for probing single molecules. This could be also used for more sensitive bioimaging techniques and monitoring real-time binding kinetics of ligand-protein binding. For biomolecular recognition in a viscous fluid, force sensitivity can be increased by decreasing the effective viscous damping. Nanoscale cantilevers are hence expected to have dramatically enhanced force sensitivity as smaller cantilevers have lower viscous damping.

In spite of the importance of nanomechanical cantilevers for ultrasensitive *in vitro* force detection, there is no widely accepted description that relates resonance frequency change to concentration or mass loading, over the entire range of viscosity relevant to biomolecular recognition in viscous fluids. In this Letter, starting with a model proposed by Sader [3], we describe the hydrodynamics of a beam, immersed in a viscous fluid, while one of its sides is entirely biofunctionalized. We generalize this model by including an additional term that takes into account the surface stress induced by the layer of mutually interacting biomolecules trapped on the functionalized part of the beam and derive its exact thermal vibrations. We find that, in air, frequency shift of the first nanoscale cantilever

mode is primarily determined by surface stress, while mass-loading effects become relevant for higher order modes. More importantly, in a viscous solution such as water, frequency shift is dominated by surface stress rather than biomolecular mass loading, contrary to conventional expectation.

Model.—Neglecting rotatory inertia, shear deformation, and internal damping, the equation of motion for the deflection $y(x, t)$ of a beam with length L , width b , and thickness d , immersed in a fluid at temperature T and loaded by a constant axial force S , is given by [3,4]

$$EI \frac{\partial^4 y}{\partial x^4} - S \frac{\partial^2 y}{\partial x^2} + \mu(x) \frac{\partial^2 y}{\partial t^2} = f_h(x, t) + f_{th}(x, t). \quad (1)$$

E and I are the Young's modulus and moment of inertia of the (coated) beam, respectively. Thermal vibrations of the beam are induced by the Brownian (Langevin) force per unit length $f_{th}(x, t)$. They are small enough for nonlinear convective inertial effects in the fluid to be neglected and for the hydrodynamic loading $f_h(x, t)$ to be linear in the beam displacement [3]. The linear mass (mass per unit length) of the system $\mu(x)$ consists of the linear mass of the beam μ_b , and the linear mass of the trapped biomolecules $\mu_l(x)$. The axial load S introduced in Eq. (1) describes the mutual interaction of biomolecules adsorbed on the beam [5]. The boundary conditions for Eq. (1) are given by $y(0, t) = y'(0, t) = 0$, $y''(L, t) = 0$, and $EIy'''(L, t) = Sy'(L, t)$, where primes denote spatial derivatives [4].

At higher concentrations, the biomolecules form a uniform layer with linear mass μ_l and thickness h so that

$$\mu(x) = \mu_b + \mu_l = \text{constant}. \quad (2)$$

The mutual interaction of biomolecules within the layer is modeled by taking into account the stress σ they generate on the coated surface of the beam. As shown in Ref. [2], this stress enables the bending of the silicon-nitride microcantilevers with length to thickness ratio L/d , ranging

from 10^2 to 10^3 . The resulting static deflection, on the order of a few tenths of microns, is related to surface stress by Stoney's formula [6]. However, for the silicon nanomechanical cantilevers under investigation here ($L/d \sim 50$), Stoney's formula typically yields angstrom-level bendings ($10^{-5} L$). So these nanocantilevers remain almost straight under the influence of surface stress. Nevertheless, as shown in [5], this stress induces an effective axial load, $S = \sigma L$, that must be included in Eq. (1). In vacuum, such a model has been studied in Ref. [7].

In addition, biomolecular interaction on the surface results in an effective Young's modulus of the layer E_l [see Ref. [8]]:

$$EI = E_b I_b + E_l I_l \simeq E_b b d^3 / 12 + E_l h b d^2 / 4. \quad (3)$$

$E_b I_b$ and $E_l I_l$ are the respective bending rigidities of the beam and the layer (the last equality holds when $h \ll d$). In the opposite limit, biomolecules with mass m sparsely scattered over the beam at locations x_i result in

$$\mu(x) = \mu_b + \mu_l(x) = \mu_b + m \sum_i \delta(x - x_i), \quad x_i \in [0, L]. \quad (4)$$

If the average spacing is large compared to their size, their mutual interaction is negligible and $S = 0$. Considering that their presence does not substantially affect the moment I_b of the beam, the bending rigidity of the whole system is the same as for an unloaded beam, $EI = E_b I_b$.

Equations of Motion.—To solve Eq. (1), we expand the deflection $y(x, t)$ and the force densities $f_h(x, t)$ and $f_{th}(x, t)$ in terms of the modes of the *bare* beam, defined as the beam without the added mass [$\mu_l(x) = 0$] though it includes the tension $S = \sigma L$:

$$y(x, t) = \sum_{n=1}^{\infty} y_n(t) \phi_n(\xi), \quad \xi = x/L. \quad (5)$$

Similar expressions hold for the force densities. The eigenmodes $\phi_n(\xi)$ satisfy the following conditions:

$$\begin{aligned} \phi_n''''(\xi) - \alpha \phi_n''(\xi) &= \beta_n^4 \phi_n(\xi); & \alpha &= \sigma L^3 / EI; \\ \phi_n(0) = \phi_n'(0) &= \phi_n''(1) = 0, & \phi_n'''(1) &= \alpha \phi_n'(1). \end{aligned} \quad (6)$$

The self-adjointness of Eq. (6) makes the modes orthonormal: $\int_0^1 \phi_n(\xi) \phi_l(\xi) d\xi = \delta_{n,l}$. From Eq. (6), the eigenvalues β_n are the successive positive roots of

$$1 + (1 + \varepsilon_n^2) \cosh \lambda_n^+ \cos \lambda_n^- + \varepsilon_n \sinh \lambda_n^+ \sin \lambda_n^- = 0, \quad (7)$$

where $\varepsilon_n = \alpha / (2\beta_n^2)$ and $\lambda_n^\pm = \beta_n [\sqrt{1 + \varepsilon_n^2} \pm \varepsilon_n]^{1/2}$. Note that, for $\varepsilon_n = \alpha / (2\beta_n^2) \ll 1$, Eq. (7) reduces to the usual clamped-free equation, $1 + \cos \beta_n \cosh \beta_n = 0$. As $\beta_n \propto n$ for large n , eigenvalues for which $n \gg \sqrt{\alpha}$ are essentially independent of the surface stress.

Let $\mu(x) = \mu_b + \mu_l(x)$. Using Eq. (5), Eq. (1) reduces to

$$M \ddot{y}_n(t) + k_n y_n(t) + \sum_{j=1}^{\infty} \Phi_{nj} \ddot{y}_j(t) = F_{n,h}(t) + F_{n,th}(t). \quad (8)$$

$M = \mu_b L$ is the mass of the beam and $F_{n,h(th)}(t) = L f_{n,h(th)}(t)$. The effective stiffness of mode n is

$$k_n = EI \beta_n^4 / L^3. \quad (9)$$

The real and symmetric matrix has components

$$\Phi_{nj} = L \int_0^1 \mu_l(\xi' L) \phi_n(\xi') \phi_j(\xi') d\xi'. \quad (10)$$

If $\mu_l(x) = \mu_l$, then $\Phi = M_l \mathbf{1}$, where $\mathbf{1}$ is the identity matrix and $M_l = L \mu_l$ is the layer mass. Equation (8) decouples and the mass of modes y_n becomes the total mass of the system, $M + M_l$. But nonuniform mass distributions as in Eq. (4) couple the bare modes of the beam.

Taking the Fourier transform of Eq. (8) and using the expression for the hydrodynamic force [9],

$$\hat{F}_{n,h}(\omega) = M_f \omega^2 \Gamma(\omega) \hat{y}_n(\omega), \quad (11)$$

where $M_f = \frac{\pi}{4} L \rho_f b^2$ is the mass of the fluid loading the beam and $\Gamma(\omega) = \Gamma_r(\omega) + i \Gamma_i(\omega)$ is a complex ‘‘hydrodynamic function’’ discussed in detail in [3], we obtain

$$\Lambda(\omega) |\hat{y}(\omega)\rangle = |\hat{F}_{th}(\omega)\rangle. \quad (12)$$

Kets $|v\rangle$ are column vectors with components v_i , $i \in \mathbb{N}$. The *non-Hermitian* matrix $\Lambda(\omega)$ is given by

$$\Lambda(\omega) = \Lambda_0(\omega) - \omega^2 \tilde{\Phi}, \quad (13)$$

where

$$\begin{aligned} \Lambda_0(\omega)_{nj} &= \{k_n - \omega^2 [M_f \Gamma(\omega) + M_n]\} \delta_{nj} \\ \tilde{\Phi}_{nj} &= \Phi_{nj} (1 - \delta_{nj}); & M_n &= M + \Phi_{nn}. \end{aligned}$$

Spectral densities.—As the *dissipative* (imaginary) part of the hydrodynamic function is frequency dependent, we apply the generalized fluctuation-dissipation theorem [10] to derive the power spectrum matrix of the stochastic forces $F_{n,th}$, $S_{\hat{F}}(\omega) = \overline{|\hat{F}_{th}(\omega)\rangle \langle \hat{F}_{th}(\omega)|}^s$ (the overline denotes thermal averaging, the superscript s refers to the spectral density, and $\langle \hat{F}_{th} \rangle$ is the Hermitian conjugate of $|\hat{F}_{th}\rangle$):

$$S_{\hat{F}}(\omega) = \frac{kT}{i\omega} [\Lambda^\dagger(\omega) - \Lambda(\omega)] = 2kTM_f \omega \Gamma_i(\omega) \mathbf{1}, \quad (14)$$

where k is the Boltzmann constant and T the temperature. In components, this yields

$$\overline{\hat{F}_{n,th}(\omega) \hat{F}_{p,th}^*(\omega')} = 2kTM_f \omega \Gamma_i(\omega) \delta_{np} \delta(\omega - \omega'). \quad (15)$$

Notice that this expression does not depend on Φ . It is the same as for a bare beam. As seen above, the stochastic forces acting on distinct modes are uncorrelated. Nevertheless, their power spectrum is not constant, contrary to the assumption made in Ref. [3], for the frequency dependence of the dissipative part of the hydrodynamic function makes them non-Markovian. Equation (15) is the generalization of the expression derived by Paul and Cross for a single cantilever mode [11]. Now, inverting Eq. (12),

we obtain

$$|\hat{y}(\omega)\rangle = \chi(\omega)|\hat{F}_{\text{th}}(\omega)\rangle, \quad \chi(\omega) = \Lambda^{-1}(\omega) \quad (16)$$

and $|\hat{y}(\omega)\rangle\langle\hat{y}(\omega)| = \chi(\omega)|\hat{F}_{\text{th}}(\omega)\rangle\langle\hat{F}_{\text{th}}(\omega)|\chi^\dagger(\omega)$. Spectral averaging the latter and using Eq. (14), we find the power spectrum matrix of the deflection modes

$$S_{\hat{y}}(\omega) = 2kTM_f\omega\Gamma_i(\omega)\chi(\omega)\chi^\dagger(\omega). \quad (17)$$

Introducing $|\phi_\xi\rangle$ with components $\phi_n(\xi)$, the Fourier transform of the deflection (5) reads $\hat{y}(x, \omega) = \langle\phi_\xi|\hat{y}(\omega)\rangle$ and using Eq. (17), we find its spectral density to be

$$\overline{|\hat{y}(x, \omega)|^2} = 2kTM_f\omega\Gamma_i(\omega) \left[\sum_{n=1}^{\infty} \frac{\phi_n^2(\xi)}{M_n^2|A_n|^2} + 2\omega^2 \sum_{n=1}^{\infty} \sum_{p=1}^{\infty} \frac{\phi_n(\xi)\phi_p(\xi)\tilde{\Phi}_{np}\Re(A_p)}{M_n^2M_p|A_n|^2|A_p|^2} + \mathcal{O}(\tilde{\Phi}^2) \right]. \quad (20)$$

In this expression, $\xi = x/L$, $\tilde{\Phi}_{np}$ is given by Eq. (14), and the quantity $A_n = \Lambda_0(\omega)_{nm}/M_n$ reads

$$A_n = \omega_n^2 - \omega^2[1 + \lambda_n\Gamma(\omega)], \quad (21)$$

where $\omega_n = \sqrt{k_n/M_n}$ is the frequency in vacuum, $\lambda_n = M_f/M_n$, and $\Re(A_n)$ is the real part of A_n . An expression similar to Eq. (20) can be derived for the slope of the deflection provided $\phi_j(\xi)$ is replaced by $\phi'_j(\xi)$ and the overall prefactor is divided by L^2 .

Expression (20) is valid for any mass distribution $\mu_i(x)$ along the beam. For a uniform layer with linear mass μ_l , $\tilde{\Phi}_{np} = L\mu_l\delta_{np}$, and then $\tilde{\Phi}_{np} = 0$. All modes have the same effective mass, $M_n = M + L\mu_l$, and are decoupled. Reinstating in Eq. (20), the second term vanishes and we obtain the *exact* spectral density of a composite beam consisting of the original beam plus the layer. For molecules trapped on the beam at positions ξ_i , the mass profile given in Eq. (4) leads to $\tilde{\Phi}_{np} = m\sum_i\phi_n(\xi_i)\phi_p(\xi_i)$ and Eq. (20) is valid up to first order in m provided the frequency satisfies $M_f\Gamma_i(\omega) \gg 4M_l$. Interestingly, if we assume N molecules to be randomly scattered along the beam in a uniform way and average $\tilde{\Phi}_{np}$ accordingly, we find $\langle\langle\tilde{\Phi}_{np}\rangle\rangle = m\sum_i\int\phi_n(\xi_i)\phi_p(\xi_i)d\xi_i = Nm\delta_{np}$. As the total mass of the trapped molecules is small compared to the mass of the beam, in the first approximation, the average spectral density is the same as the spectral density of their average mass distribution—i.e., the spectral density of a uniform layer of mass Nm .

In Fig. 1, we compare the bare beam ($\tilde{\Phi} = 0$) spectral density of the deflection slope at the tip of a rectangular silicon nanocantilever ($E = 160$ GPa, $\rho = 2.33 \times 10^3$ kg/m³) to Sader's result [3] in air and water. The beam dimensions are $d \times b \times L = 0.2 \times 0.2 \times 10$ μm . From [13], at $T = 27$ °C, the viscosities are $\eta_{\text{air}} = 1.86 \times 10^{-5}$, $\eta_{\text{water}} = 8.59 \times 10^{-4}$ kg/(m.s) and the densities are $\rho_{\text{air}} = 1.18$, $\rho_{\text{water}} = 997$ kg/m³. Typical values for the Reynolds number defined as [3] $\text{Re} = \rho_f b^2 \omega / 4\eta$ are $\text{Re}_{\text{air}} \simeq 0.01$ and $\text{Re}_{\text{water}} \simeq 0.036$ at resonance. Although different, Sader's formula can be shown to reduce to (20) provided $\lambda|\Gamma(\omega)| \ll 1$. This explains why the results are

$$\overline{|\hat{y}(x, \omega)|^2} = 2kTM_f\omega\Gamma_i(\omega)\langle\phi_\xi|\chi(\omega)\chi^\dagger(\omega)|\phi_\xi\rangle. \quad (18)$$

The total mass of the particles trapped on the beam M_l is small compared to the mass of the beam. This justifies treating $\omega^2\tilde{\Phi}$ perturbatively provided its elements stay small compared to the diagonal elements of $\Lambda_0(\omega)$. This is indeed the case [12] provided $M_f\Gamma_i(\omega) \gg 4M_l$. By inverting Eq. (13), we obtain in first order in $\tilde{\Phi}$

$$\chi\chi^\dagger = \chi_0\chi_0^\dagger + \omega^2\chi_0(\tilde{\Phi}\chi_0 + \chi_0^\dagger\tilde{\Phi})\chi_0^\dagger + \mathcal{O}(\tilde{\Phi}^2), \quad (19)$$

where $\chi_0 = \Lambda_0^{-1}$. Reinstating in Eq. (18), we finally get

very similar in air [$\lambda|\Gamma(\omega)| \simeq 0.06$ at resonance] while they start to differ in water [$\lambda|\Gamma(\omega)| \simeq 25$ at resonance].

Frequency shift.—As stated earlier, when trapped molecules form a uniform layer, the *exact* spectral density of the beam deflection is given by

$$\overline{|\hat{y}(x, \omega)|^2} = \frac{2kTM_f\omega\Gamma_i(\omega)}{(M + M_l)^2} \sum_{n=1}^{\infty} \frac{\phi_n^2(\xi)}{|A_n|^2}, \quad (22)$$

where M_l is the mass of the layer and where A_n is given in Eq. (21) with $M_n = M + M_l$. When the peaks of Eq. (22) are sharp enough, the hydrodynamic function is almost constant in their vicinity and the resonant frequency satisfies the self-consistent equation:

$$\omega_{R,n}^2 = f(\omega_{R,n}, M_n)k_n, \quad f = \frac{1}{3} \frac{R + \sqrt{4R^2 + 3I^2}}{R^2 + I^2}, \quad (23)$$

where $R = M_n + M_f\Gamma_r$, $I = M_f\Gamma_i$, and $\Gamma_{r,i} \equiv \Gamma_{r,i}(\omega_{R,n})$. From the expression (23), the mass and stiffness variations due to the layer, δM and δk_n , induce a relative frequency shift between a bare and a loaded beam:

$$\frac{\delta\omega_{R,n}}{\omega_{R,n}} = \frac{1}{2 - \omega_{R,n} \frac{\partial \ln f}{\partial \omega_{R,n}}} \left[\frac{\delta k_n}{k_n} + \frac{\partial \ln f}{\partial M} \delta M \right]. \quad (24)$$

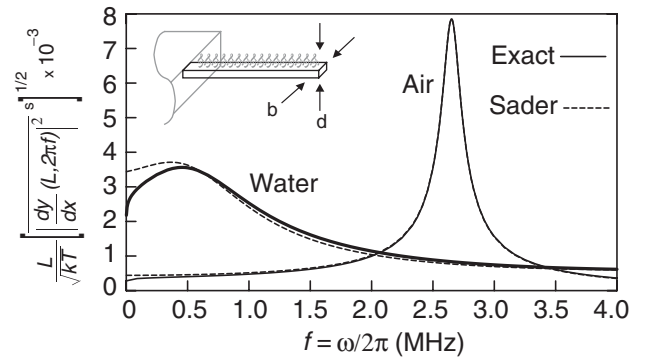


FIG. 1. Inset: schematic diagram of the beam with a layer of molecules on its functionalized side. Main figure: exact spectral density of the deflection slope of a silicon nanobeam without molecular layer. Calculations done in air and water (solid lines) compared to Sader's results [3] (dashed lines).

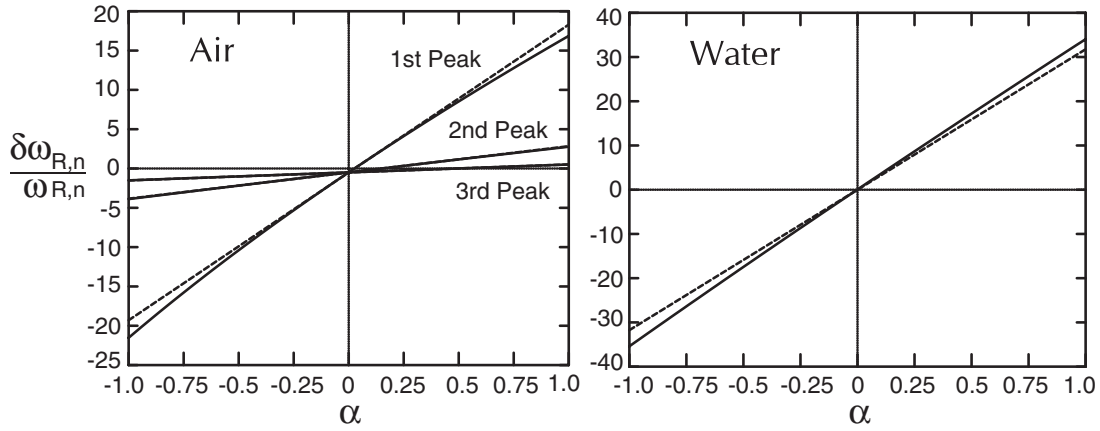


FIG. 2. Relative frequency shift (in %) in air and water vs the dimensionless stress, $\alpha = \sigma L^3/EI$. $M_l = M/100$ and $E_l = 0$. Other parameters are the same as in Fig. 1. Solid line: exact result from Eq. (22). Dotted line: linear approximation from Eqs. (24) and (25).

Here, $\delta M = M_l$ and its prefactor in Eq. (24) takes into account dissipative ($M_f \Gamma_i$) and fluid mass loading ($M_f \Gamma_r$) effects. According to (9), the two contributions to the stiffness δk_n come from the bending rigidity, $E_b I_b \rightarrow E_b I_b + E_l I_l$, and from the surface stress through the eigenvalue $\beta_n(\alpha)$. From Eqs. (3) and (7), we find

$$\frac{\delta k_n}{k_n} = \frac{3hE_l}{dE_b} + \frac{2T_n t_n + \beta_{0,n}(T_n + t_n)}{\beta_{0,n}^3(t_n - T_n)} \alpha, \quad (25)$$

where $\beta_{0,n}$ is the n th root of $\cosh(\beta) \cos(\beta) + 1 = 0$ and where $T_n = \tanh \beta_{0,n}$, $t_n = \tan \beta_{0,n}$. The last term of (25) has been obtained from (7) in perturbation. It is valid when $\alpha \ll n^2$ and vanishes as $n \rightarrow \infty$.

Using the same data as in Fig. 1, we display in Fig. 2 the relative frequency shift in air (left) and water (right) versus the dimensionless surface stress α . The exact shift is evaluated from the spectral density in Eq. (22) and compared to its linear approximation in Eq. (24). The layer mass has been arbitrarily fixed to 1% of the beam mass and E_l set to zero, hence the negative offset observed in air at $\alpha = 0$. For typical values of the surface stress, $\sigma \sim 10^{-2} \text{ J m}^{-2}$ [see Wu *et al.* in Ref. [2]], $|\alpha| \lesssim 1$. In air, $\lambda |\Gamma(\omega_{R,n})| \ll 1$, and $f \sim 1/M$. Then, $\partial \ln f / \partial M \sim -1/M$, $\partial \ln f / \partial \omega_{R,n} \sim 0$, and we recover the usual frequency shift for a linear oscillator in vacuum. As seen on the left panel, the first peak is the most sensitive to α . The deviation of the data from the linear result in Eq. (25) indicates that the condition $\alpha \ll n^2$ with $n = 1$ becomes violated. This effect disappears for the second and third peaks that are less sensitive to α . In water (right panel), a single broad peak occurs. Equation (23) loses its accuracy but the frequency shift in Eq. (24) derived from it is still acceptable. The contribution of $\partial \ln f / \partial M$ becomes negligible while $\partial \ln f / \partial \omega_{R,n} \sim -\partial \ln \Gamma_i / \partial \omega_{R,n}$ becomes important, hence the increase in the slope of the relative frequency shift versus α in water compared to air.

In conclusion, we treat the thermal response of biofunctionalized nanocantilevers with a generalized fluctuation-dissipation relation. In a viscous fluid like water, the reso-

nance frequency shift for a continuous distribution of biomolecules on the cantilever surface is found to be dominated by surface stress rather than the mass loading of biomolecules.

We acknowledge support by the Department of Defense MSRP program (W81XWH-04-1-0578) and the National Science Foundation (DBI-0242697).

*Present address: University of Pittsburgh MSTP, 526 Scaife Hall, 3550 Terrace Street, Pittsburgh, PA 15261.

- [1] M. B. Viani *et al.*, J. Appl. Phys. **86**, 2258 (1999).
- [2] G. Wu *et al.*, Nat. Biotechnol. **19**, 856 (2001); Proc. Natl. Acad. Sci. U.S.A. **98**, 1560 (2001).
- [3] J. E. Sader, J. Appl. Phys. **84**, 64 (1998); C. P. Green and J. E. Sader, J. Appl. Phys. **98**, 114913 (2005).
- [4] J. L. Humar, *Dynamics of Structures* (Prentice-Hall, Englewood Cliffs, NJ, 1990), p. 654.
- [5] G. Y. Chen *et al.*, J. Appl. Phys. **77**, 3618 (1995); P. Müller and R. Kern, Surf. Sci. **301**, 386 (1994).
- [6] G. Stoney, Proc. R. Soc. A **82**, 172 (1909); J. E. Sader, J. Appl. Phys. **89**, 2911 (2001).
- [7] P. Lu *et al.*, Mater. Phys. Mech. **4**, 51 (2001); Q. Ren and Y.-P. Zhao, Microsystem Technologies **10**, 307 (2004).
- [8] J. P. Gere and S. P. Timoshenko, *Mechanics of Materials* (PWS Publishing Company, Boston, 1997).
- [9] L. Rosenhead, *Laminar Boundary Layers* (Clarendon, Oxford, 1963), p. 391; We assume here that the presence of a layer of molecules binding to the beam does not affect the hydrodynamic force.
- [10] N. Smith, J. Appl. Phys. **90**, 5768 (2001); **92**, 3877 (2002).
- [11] M. R. Paul and M. C. Cross, Phys. Rev. Lett. **92**, 235501 (2004).
- [12] As $\Gamma_i(\omega) \rightarrow 0$ when $\omega \rightarrow \infty$, $M_f \Gamma_i(\omega) \gg 4M_l$ is violated at some critical frequency beyond which Eq. (19) does not hold. A “nonperturbative” treatment of the inversion of $\Lambda(\omega)$ is then in order. It can be done approximately by analytically inverting the 2×2 or 3×3 sub-block of $\Lambda(\omega)$ surrounding the small diagonal element.
- [13] J. W. M. Chon, P. Mulvaney, and J. E. Sader, J. Appl. Phys. **87**, 3978 (2000).